Special Issue

Multimodal Imaging Patterns for Development of Central Atrophy Secondary to Age-Related Macular Degeneration

Sarah Thiele, Maximilian Pfau, Petra P. Larsen, Monika Fleckenstein, Frank G. Holz, and Steffen Schmitz-Valckenberg

Department of Ophthalmology, University of Bonn, Bonn, Germany

Correspondence: Steffen Schmitz-Valckenberg, Department of Ophthalmology, University of Bonn, Ernst-Abbe-Str. 2, 53127 Bonn, Germany; steffen.schmitz-valckenberg@ukbonn.de.

Submitted: November 7, 2017
Accepted: January 22, 2018

Citation: Thiele S, Pfau M, Larsen PP, Fleckenstein M, Holz FG, Schmitz-Valckenberg S. Multimodal imaging patterns for development of central atrophy secondary to age-related macular degeneration. *Invest Ophthalmol Vis Sci*. 2018;59:AMD1–AMD11. https://doi.org/10.1167/iovs.17-23315

Purpose. To evaluate the development of central atrophy in eyes with age-related macular degeneration (AMD).

Methods. Six-year longitudinal multimodal retinal imaging data (MODIAMD study) from 98 eyes of 98 subjects with non–late-stage AMD in the study eye at baseline were analyzed for the presence of central atrophy at each annual follow-up visit. Development, manifestation, and further progression of complete retinal pigment epithelium and outer retinal atrophy (cRORA) by multimodal imaging data were compared with atrophy detection based on color fundus photography only.

Results. Seventeen study eyes with development of central cRORA within 6 years (cumulative rate: 17.4%) were identified based on multimodal imaging. In 10 (60%) of these eyes, presence of central manifest atrophy was initially not detectable by color fundus photography. In six (35%) eyes, central cRORA occurred by the spread of existing paracentral atrophy toward the fovea. Drusen-associated atrophy development was noted in eight eyes. In two eyes, atrophy development was associated with refractile deposits, while only pigmentary changes in absence of large drusen or refractile deposits were detectable before atrophy occurrence in one eye.

Conclusions. The earlier and more precise detection of central cRORA by multimodal imaging as compared to atrophy detection solely based on color fundus photography allows for more accurate detection and identification of different pathways for atrophy development. In accordance with previous clinical and histopathologic reports, the results confirm that different precursor lesions may independently proceed to central cRORA in AMD.

Keywords: conversion, multimodal imaging, biomarker, geographic atrophy, image analysis

Development of retinal atrophy involving photoreceptors and the retinal pigment epithelium (RPE) is a major cause for irreversible visual loss and legal blindness. Over 5 million people worldwide are affected by "geographic atrophy," the nonexudative late-stage manifestation of age-related macular degeneration (AMD).[1] The impact of atrophy on irreversible visual loss is also increasingly relevant for exudative AMD forms, as progressive atrophy manifestation is observed in eyes undergoing repeated intravitreal injection of anti-vascular growth factor (VEGF) inhibitors for treatment of choroidal neovascularizations (CNV).[2–6]

Geographic atrophy (GA) is characterized by progressive degeneration of photoreceptors, the RPE, and the choriocapillaris in the setting of extensive and characteristic extracellular deposits.[7–11] Extensive research in the past has been focused on the manifestation and progression, that is, enlargement of GA.[12–14] Different subphenotypes and prognostic factors for disease progression have been identified, particularly along with the advent of high-resolution imaging modalities.[15,16] Recently, several large-scale clinical studies have been initiated and completed, aiming to halt or slow GA lesion enlargement.[17–19] Typically, the minimum total atrophic lesion size for inclusion in clinical studies in GA is currently 0.5 to 1.0 disc areas (1.25–2.5 mm^2).

The natural history of atrophy development itself, that is, before the presence of GA with a minimum total lesion of 0.5 disc areas, has been studied in detail by using color fundus photography (CFP). Large drusen (diameter: >125 μm), hyperpigmentary and hypopigmentary changes, and refractile/crystalline deposits have been described as potential precursor lesions.[4,20–22] In a clinicopathologic study, Sarks et al.[7] distinguished three patterns of atrophy evolution: (1) primary age-related atrophy (no obvious association with drusen), (2) drusen-related atrophy (association with regressing drusen or drusen clusters), and (3) other causes (e.g., resolution of pigment epithelial detachment). Furthermore, the Age-Related Eye Disease studies (AREDS 1 and AREDS 2) have reported the development of atrophy based on definitions by CFP in eyes with early and intermediate AMD (iAMD).[21,23] While CFP assessment has been established as the gold standard in clinical AMD trials, the ability to detect early stages of atrophy and precursor lesions is challenging due to low contrast and limited resolution.[24] Using high-resolution multimodal imaging, in particular spectral-domain optical coherence tomography (SD-OCT) and confocal scanning laser ophthalmoscopy (cSLO) fundus autofluorescence (FAF), the evolution of atrophy has been scrutinized in more detail.[23,25–28] Among those observations, "nascent GA" as part of the chronological appearance of drusen-associated atrophy development has been analyzed by

Wu et al.[26] Recently, the Classification of Atrophy Meetings (CAM) group defined OCT-based criteria for complete RPE and outer retinal atrophy (cRORA) as atrophy in AMD.[29]

The aim of the current study was to analyze the incidence and development of central atrophy in AMD eyes that were considered at high risk for development of late AMD stages. Hereby, the term "central" referred to the presence of atrophy within the central subfield of the Early Treatment in Diabetic Retinopathy Study (ETDRS) grid. Three different definitions for central "atrophy" were employed: presence of atrophy according to CFP-based criteria only by using two different definitions for minimal lesion size, and thirdly, presence of cRORA according to OCT-based criteria as recently published by the CAM initiative and also confirmed by additional imaging modalities including cSLO-FAF.

The analysis was performed in eyes that had been prospectively observed over 6 years by multimodal retinal imaging.

Methods

Study Cohort

The Molecular Diagnostics of Age-related Macular Degeneration (MODIAMD) Study (www.modiamd.de, available in the public domain) is a prospective, noninterventional, observational, monocenter longitudinal natural history study in patients at high risk for developing late-stage AMD in the study eye. Patients were recruited between November 2010 and September 2011 at the Department of Ophthalmology, University of Bonn, Bonn, Germany. The study followed the tenets of the Declaration of Helsinki and was approved by the local ethics committee (Ethik-Kommission der Universität Bonn Lfd-Nr: 175/10). Informed consent was obtained from each patient after explanation of the nature and possible consequences of the study. Subjects underwent annual examinations including measurement of best-corrected visual acuity (BCVA) using Early Treatment Diabetic Retinopathy Study (ETDRS) charts and extensive retinal imaging. The study is still ongoing. The details of the initial study design have been described in previous reports.[30,31] Briefly, 98 patients $>$ 50 years of age and with retinal changes classified as AREDS 3 or 4 (based on AREDS report no. 6) (i.e., having at least one eye without advanced AMD that would be considered to be at high risk for developing late stages of the disease) were enrolled.[32] According to the study protocol, subjects exited the study in the case of conversion to late-stage AMD (i.e., development of either central atrophy or CNV). For the current analysis, the database was screened after completion of 6 years of follow-up (seven study visits: baseline and six follow-up visits) of the MODIAMD cohort. All study eyes (i.e., no advanced AMD at baseline) that had converted to central atrophy since baseline were identified.

Imaging Protocol

Multimodal imaging was performed at each visit according to standardized operating procedures as previously described.[22,30,33] After dilation of pupils with 1.0% tropicamide, CFP were recorded using the Visucam 500 (Carl Zeiss Meditec AG, Jena, Germany). Additionally, CFP was performed with a field of 45° $\times$ 45° and centered to the fovea.

Combined and simultaneous cSLO+SD-OCT imaging (768 $\times$ 768 pixels) was performed (Spectralis HRA+OCT; Heidelberg Engineering, Heidelberg, Germany) with acquisition of central 30° $\times$ 30° near-infrared reflectance (NIR, λ = 820 nm, Automatic Real Time [ART] at least 15 frames) and fundus autofluorescence with both blue-light excitation (BAF, exc. λ = 488 nm, em. λ = 500–800 nm, at least 15 frames) and green-light excitation (GAF, exc. λ = 514 nm, em. λ = 500–800 nm, at least 15 frames).

Definitions and Grading

According to the MODIAMD study protocol, development of central atrophy was originally defined using a multimodal imaging approach that aimed to consider the existing AREDS definition in combination of findings made by imaging modalities beyond CFP. For the current analysis, the definition based on multimodal imaging was adopted to the recent consensus classification system of cRORA by the CAM initiative. Further, two definitions solely based on CFP were employed for presence of central atrophy (Table 1).

Based on CFP, atrophy was defined as a sharply demarcated, usually circular zone of partial or complete depigmentation of the RPE, typically with exposure of underlying large choroidal blood vessels and with no clear or suspicious signs of active or regressed CNV.[32] Two different minimal lesion size criteria were used. First, derived from the initial AREDS definition from 2001, the lesion had to be equal to or larger than circle I-1, corresponding to one-eighth disc diameter or 188 μm in diameter (CFP-I).[32] Second, derived from the revised definition (as introduced in 2013), the lesion had to be at least as large as circle I-2, corresponding to one-fourth disc diameter or 450 μm in diameter, also taking into account the change in size of the standard disc area from 1500 to 1800 μm (CFP-II).[34,35]

Finally, based on findings by multimodal imaging, development of central atrophy was defined as the presence of cRORA. These included the following specific OCT-based criteria: (1) region of hypertransmission of at least 250 μm in diameter; (2) a zone of attenuation or disruption of the RPE of at least 250 μm in diameter; (3) evidence of overlying photoreceptor degeneration including loss of the interdigitation zone, ellipsoid zone, and external limiting membrane as well as thinning of the outer nuclear layer; and (4) absence of scrolled RPE or other signs of RPE tear. Further, a retinal area with a markedly reduced FAF signal and a minimum lesion size of 0.05 mm^2 as quantified by RegionFinder software (Heidelberg Engineering) had to be present. The individual lesion had to be spatially confined to either complete or incomplete depigmentation or other AMD typical changes (e.g., hyperpigmentation, crystalline deposits) on CFP, provided that any hemorrhages or exudates were absent. Further, no leakage had to be present on fluorescein angiography (FA) or any other signs of exudation by other modalities.

For each of these three definitions of atrophy, the atrophy was defined to be "central atrophy" if any part of the atrophy was within the central subfield of the ETDRS grid. Hereby, the centration of the ETDRS grid on the foveal center was verified and, if indicated, manually corrected for each modality and at each visit. To identify the foveal center, the distribution of macular pigment and the shape of the retinal vessels (assuming the foveal center to be approximately 15° temporal and approximately 0.5° inferior to the center of the optic nerve head) were used as landmarks. Further, the dense raster SD-OCT scan was reviewed to identify the center of the foveal depression with the closest contact of the outer nuclear layer to the vitreoretinal interface. For description of SD-OCT layers, the nomenclature according to the proposed lexicon for anatomic landmarks was used.[36] Reticular drusen (RDR) were characterized as a group of hyporeflective dots, targets, or a ribbon pattern in cSLO NIR images and as hyperreflective mounds above the RPE in SD-OCT images.[31,37,38]

All available imaging data at each visit were carefully reviewed and evaluated for development of central atrophy

Table 1. Criteria for the Three Definitions of Central Retinal Atrophy

Definition	CFP-I	CFP-II	Multimodal
Modalities	Clinical examination and CFP		FAF, SD-OCT, NIR, CFP, FA*
Qualitative features*	• VSharply demarcated, usually circular zone of partial or complete depigmentation of the RPE • Typically with exposure of underlying large choroidal blood vessels • No clear or suspicious signs of active or regressed choroidal neovascularization		• Complete RPE and outer retinal atrophy (cRORA) based on OCT criteria 1. Region of hypertransmission of ≥250 μm in diameter 2. Zone of attenuation or disruption of the RPE of ≥250 μm in diameter 3. Evidence of overlying photoreceptor degeneration 4. Absence of scrolled RPE or other signs of RPE tear • Correlation to a sharply demarcated area with severely reduced FAF signal ≥0.05 mm^2 • Spatially confined to either complete or incomplete depigmentation or other AMD typical changes by CFP (including hyperpigmentary changes and crystalline deposits) • Exclusion of any hemorrhages or exudates by CFP • No leakage by FA or any other signs of exudation by any modality
Minimal lesion size	Diameter of 188 μm	Diameter of 450 μm	Diameter of 250 μm
Scaling	Disc size as reference assuming standard diameter of 1500 μm	Disc size as reference assuming standard diameter of 1800 μm	Scaling of Heidelberg Eye Explorer
Configuration	At least one lesion (either uni- or multifocal)		
Location	Any part of the lesion within the central subfield of the ETDRS grid		

* All of the listed criteria need to be present.

according to each of the three definitions by two of the authors (ST and SSV). In a further session among all authors, the identified cases were reviewed, including all available imaging data, and then discussed for different patterns and precursor lesions of atrophy development.

Results

A total of 17 patients (17.4%) developed central atrophy in the study eye at year 6, based on the cRORA definition by multimodal imaging. There were 15 females and nine right eyes. The mean age and BCVA at baseline of these subjects was 72.8 ± 6.8 years (mean ± SD; range, 56–89) and 77.4 ± 5.6 ETDRS letters (range, 65–85), respectively. Four of the 17 patients were categorized as AREDS 3 at baseline. Nine of these 17 patients (53%) presented RDR at baseline, while no direct spatial association of RDR and atrophy development was evident.

Of the remaining 81 of 98 patients who did not develop central cRORA in the study eye, CNV occurred in 29 (29.6%) study eyes (21 females, at baseline: age 73.03 ± 7.15 years, BCVA 76.93 ± 8.64 ETDRS letters). In 20 study eyes, there were still no signs of either central cRORA or CNV (15 females, at baseline: age 69.15 ± 6.76 years, BCVA 79.95 ± 6.92 ETDRS letters). A total of 32 (32.7%) patients (17 females, at baseline: age 76.75 ± 6.82 years, BCVA 78.06 ± 5.8 ETDRS letters) had exited the study (5 missing for year 1, 10 for year 2, 17 for year 3, 26 for year 4, 30 for year 5) for various reasons (withdrawal of consent 22, death 1, poor health 9). For a flowchart of the MODIAMD study cohort, see Supplementary Figure S1.

The further analysis of the 17 eyes with development of central cRORA disclosed a mean BCVA of 70.7 ± 15.4 ETDRS letters for each eye at the first study visit when central atrophy was identified. The mean change of BCVA at this visit compared to baseline was –6.71 ± 16.1 ETDRS letters.

Table 2 lists the cumulative number of eyes at each study visit with presence of central atrophy, separately for the three definitions. Overall, a higher number of eyes with development of central atrophy was detected at each of the six follow-up visits by the multimodal imaging data set as compared to both CFP definitions. If central atrophy was present according to CFP, it was always also detected by multimodal imaging.

Within the subgroup of 10 eyes with earlier detection by multimodal versus CFP definitions, further longitudinal data were available for four eyes that had been obtained outside the study as part of routine clinical care. In one eye, central atrophy according to both CFP-I and CFP-II definitions developed 11 months later. Another single eye had developed CNV before atrophy was evident in CFP, and two eyes had not yet developed central manifest atrophy according to CFP, respectively. For the remaining six eyes, no follow-up data after development of central atrophy according to the multimodal definition were available ($n = 2$ at follow-up 2, $n = 3$ at follow-up 4, and $n = 6$ at follow-up 5).

All available imaging data were reviewed of the 17 eyes that had been determined out of the MODIAMD study cohort with development of central cRORA within 6 years. Hereby, the following different phenotypic patterns were identified.

In six eyes, central atrophy occurred as a spread of preexisting paracentral atrophy toward the fovea (type 1) (i.e., presence of atrophy without involvement of the central ETDRS subfield at baseline and inclusion of that subfield during the observational period). In the remaining 11 study eyes, three distinct precursor lesions and patterns for de novo development of central cRORA were identified: (1) drusen-associated ("nascent GA") (type 2a), (2) association with pigmentary changes without presence of large drusen (type 2b), and (3) association with refractile deposits (type 2c).

Type 1: Spread of Existing Paracentral Atrophy Toward the Fovea

The mean total lesion size of paracentral atrophy at baseline, that is, sparing of the central subfield of the ETDRS grid, of the six eyes with preexisting noncentral atrophy was 0.97 ± 0.69 mm^2 (mean ± SD, range, 0.11–1.88) using the RegionFinder

Table 2. Cumulative Number of Study Eyes at Each Study Visit

	Baseline	Year 1	Year 2	Year 3	Year 4	Year 5	Year 6
Number of Subjects							
Total	98	86	68	55	38	26	20
Exit because of CNV	0	2	11	15	19	25	29
Exit because of dropout and no conversion into late AMD	0	5	10	17	26	30	32
Presence of Central Manifest Atrophy							
Multimodal	0	5	9	11	15	17	17
CFP-I	0	3	6	6+1*	6+1*	6+1*	6+1*
CFP-II	0	3	6	6+1*	6+1*	6+1*	6+1*

* According to the study protocol, subjects exited the study in case of conversion to late-stage AMD (i.e., development of either central atrophy or choroidal neovascularization based on definitions by multimodal imaging). For one study eye with earlier central atrophy development by multimodal imaging and then followed by CFP definitions, further longitudinal data were available that had been obtained outside the study as part of routine clinical care.

software and based on combined assessment of FAF and NIR cSLO imaging.[16,39] In accordance with the wide range of total lesion sizes, variable configurations of atrophic patches with sparing of the fovea were noted. Coalescence of multifocal patches and characteristic SD-OCT findings at the perilesional atrophic zone were observed as previously described, including hyporeflective wedge-shaped bands, migration of hyperreflective material, and changes in drusen height.[26,40] For assessment of foveal involvement, use of NIR cSLO and SD-OCT imaging was particularly helpful in addition to FAF images, as distinction of macular pigment versus atrophy was challenging when using the latter modality alone. Multimodal imaging (i.e., NIR and SD-OCT) was also felt to be helpful for accurate identification of the foveal center point and thus verifying and, if indicated, correcting the centration of the ETDRS grid as compared to solely using CFP for exact assessment of atrophy involvement of the central subfield. In addition to paracentral atrophy at baseline, all six eyes exhibited RDR. Figure 1 shows a typical example of this pattern for development of central atrophy.

Type 2a: Drusen-Associated Development of Central Atrophy

In eight eyes, development of central atrophy in association with large confluent drusen was observed. The characteristic features for this pattern, previously described as "nascent GA," were noted before presence of atrophy, including subsidence of the outer plexiform layer (OPL) and inner nuclear layer (INL), disruption of the RPE band, breaks in the external limiting membrane (ELM), and traces of choroidal hypertransmission as well as development of a hyporeflective wedge-shaped band along with drusen regression. While all eight eyes showed hyperpigmentary changes in CFP analysis, hyperreflective foci (HRF) toward the inner retinal layers were observed in only six eyes by SD-OCT imaging. RDR were detectable in two of the eight eyes before atrophy, while atrophy development itself was not spatially confined to the presence of RDR. By FAF imaging, localized severe signal alterations with levels of increased intensities were observed at the site of drusen regression and before presence of central atrophy. Of note, no marked changes of the FAF signal were observed at the site of other drusen in the same eye that did not develop atrophy within the observational period (Fig. 2).

Type 2b: Association With Pigmentary Changes Without Presence of Large Drusen

Development of central atrophy without the colocalization of large drusen at any time point was identified in one eye (Fig. 3). By CFP, a hyperpigmentary laminar lesion surrounded by a hypopigmentary circle was initially observed that was spatially confined to a "patchy FAF pattern" showing abnormal signal intensities with mainly levels of increased FAF. At the same time, SD-OCT showed hyperreflective material above the RPE/Bruch's membrane band and widening of the RPE/Bruch's membrane complex, as well as of the interdigitation and ellipsoid zones, while ELM still showed no disruption. Drusen material was limited to small- or intermediate-size drusen. No RDR were detectable in this eye. During further follow-up, hyperpigmentary deposits transformed to multiple smaller hyperpigmentary lesions, showing a "speckled appearance" by CFP. Irregular FAF abnormal intensities changed, evolving to more and more areas of decreased FAF. A rather irregular area of abnormal FAF was noted before development of central atrophy within the lesion area; that is, atrophy did not evolve as a small, sharply demarcated zone of homogenous decreased FAF and then further spread to neighboring retina as is usually seen in larger atrophic areas in advanced atrophic AMD. SD-OCT showed beginning disruption of outer retinal layers, including the ELM, as well as localized thinning but not complete loss of the outer nuclear layer and traces of choroidal hypertransmission. During further follow-up, progressive thinning and disruption of outer retinal layer by OCT as well as increasing focal levels of decreased FAF were noted. It appeared that focal areas of atrophy within the initial lesion occurred first before the entire lesion developed the typical features of atrophy according to the three definitions.

Type 2c: Association With Refractile Deposits

There were two eyes in which central atrophy developed in association with refractile deposits but no local occurrence of large drusen (Fig. 4). Refractile deposits as precursor lesions showed a glistening and yellow-shiny appearance in CFP. By NIR imaging, a corresponding hyperreflective appearance was detected.[22] FAF imaging showed mildly increased intensities or a mottled signal that evolved over time to levels of decreased FAF intensities. The distinctive feature as seen by SD-OCT imaging was a laminar intense hyperreflectivity at the level of Bruch's membrane or a pyramidal structure at the level of the outer retina ("ghost drusen").[22,41,42] One of the two eyes with refractile deposits presented RDR, while the presence of refractile deposits and the local atrophy development appeared not to be spatially associated with RDR presence. Further, progressive disruption of outer retinal bands by SD-OCT was noted. SD-OCT imaging showed fading of the laminar hyperreflectivity and a dip of the ELM and outer nuclear layer (ONL) loss along with the occurrence of traces of choroidal hypertransmission.

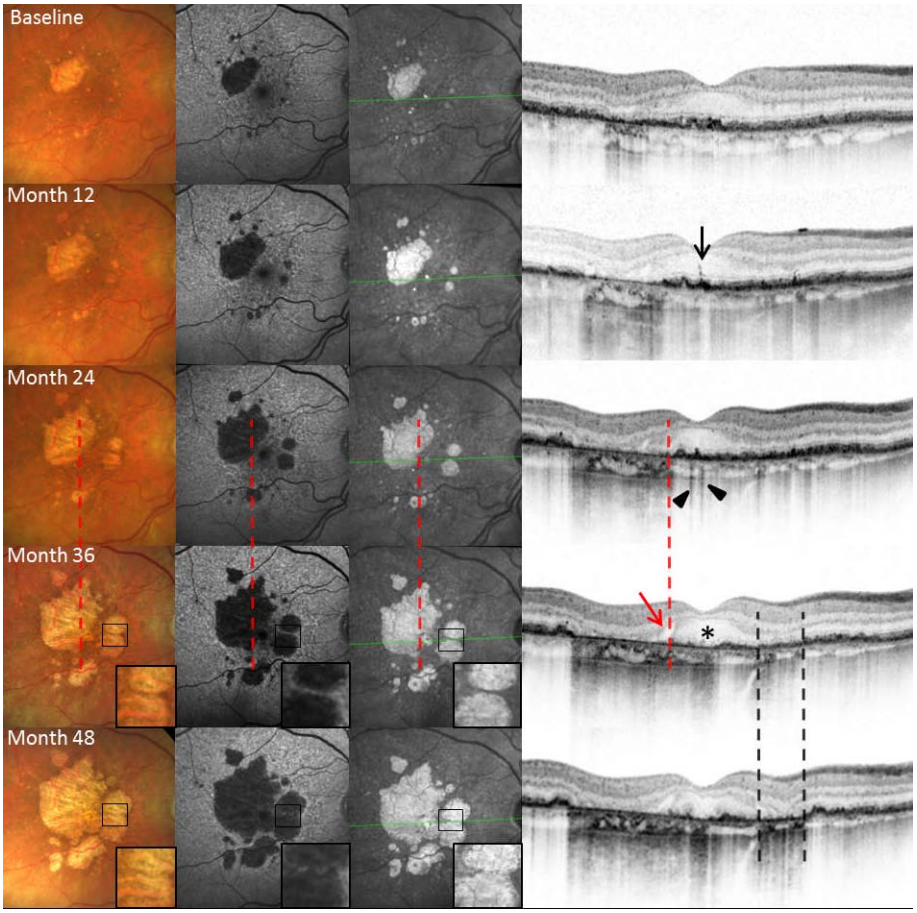

FIGURE 1. Typical example (type 1) for existing paracentral retinal atrophy at baseline (*first row*) with subsequent involvement of the fovea at later visits (*second to fifth rows*: subsequent annual follow-up visits), as shown by multimodal imaging (*for each row from left to right*: color fundus photography, confocal scanning laser ophthalmoscopy fundus autofluorescence, combined confocal scanning laser ophthalmoscopy NIR and spectral-domain optical coherence tomography). Perilesional zone of atrophy indicates the spread of atrophy (month 24 and 36: *red dashed lines*) with subsequent foveal involvement, which is well apparent in the SD-OCT image (month 36: *black star*). Please note the lateral spread of choroidal hypertransmission from temporal to nasal. Hyperreflective foci (*black arrow* at month 12) in foveal region are followed by a focal hypertransmission of SD-OCT signal into the choroid 1 year later (month 24: *black arrowheads*) indicating a disrupted RPE. At month 36, atrophy has involved the fovea with loss of the external limiting membrane, the ellipsoid zone, and RPE (*black star*). Hyporeflective wedge-shaped bands in the context of drusen-associated atrophy development are marked in SD-OCT images at month 36 (*red arrow*). Coalescence of two atrophic lesions is detectable in CFP, NIR, and FAF images between month 36 and 48 (*black boxes*). Corresponding area of atrophy coalescence is marked in SD-OCT at month 36 and 48 (*black dashed lines*).

Development of Central Atrophy in the Fellow Eye

Of the 23 study patients with AREDS 3 at baseline, conversion to central atrophy at follow-up year 6 had occurred in a total of three fellow eyes according to the multimodal definition and both CFP definitions. Development of central atrophy was associated with retinal hyperpigmentation (type 2b) without the presence of drusen at baseline ($n = 1$) and enlargement of preexisting paracentral atrophy (type 1) with foveal involvement ($n = 1$).

In the third eye, development of central atrophy was associated with flattening of a large serous pigment epithelium detachment (PED) (Fig. 5). In this example, confluent drusen with ill-defined hypopigmentary changes and central hyperpigmentary clumping were seen by CFP at baseline.[43] FAF imaging showed a cartwheel-like configuration with levels of increased and decreased signal intensities. Hyperreflective irregularities were visible by NIR imaging. On SD-OCT imaging, a dome-shaped elevation of the RPE along with HRF in inner and outer retinal layer, corresponding to pigment clumping, was detected. Fluorescein angiography did not show any leakage or evidence for CNV at baseline (not shown).

Over time, coalescence of brownish pigment clumps, as seen by CFP, was associated with progressive development of FAF abnormalities with, especially, levels of decreased intensities and hyperreflective irregularities by NIR, respectively. SD-OCT imaging showed an initial increase of both height and diameter of the PED. Progressive disruption of outer retinal layers and the RPE occurred. These gaps in the RPE were associated with an initial faint hyperreflective signal below the RPE. Finally, the number of the HRF within retinal layers decreased.

At year 3, a sharply demarcated area of decreased intensities was detectable by FAF imaging in the center of the lesion, resembling the typical appearance of an atrophic area. The borders of this lesion were also traceable by CFP and NIR. In OCT, a progressive disruption of the RPE was visible. The area of the lesion, as seen by en face imaging, corresponded to a strong hyperreflectivity below the RPE. This latter signal resembles the typical signal intensities of choroidal hyper-

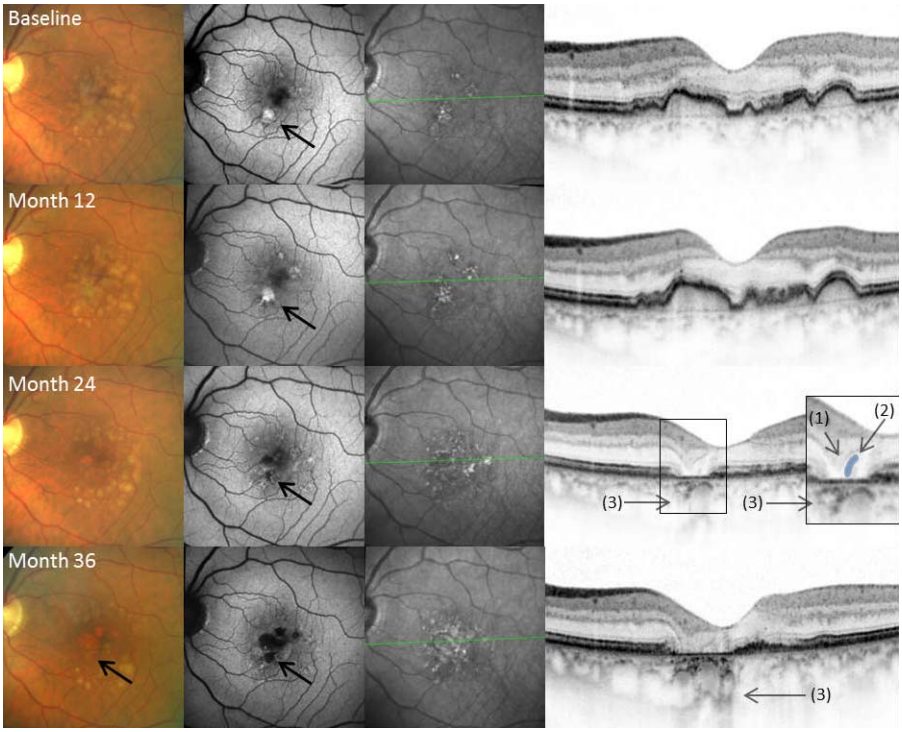

Figure 2. Representative example for drusen-associated development of central atrophy (type 2a). Same arrangement of images as in Figure 1. At month 24, development of drusen-associated atrophy ("nascent GA") is commencing with subsidence of the outer plexiform and inner nuclear layer (**1**) and formation of a hyporeflective wedge-shaped band (here illustrated with *blue-marked overlay* [**2**]) and choroidal hypertransmission of SD-OCT signal (**3**). At month 36, choroidal hypertransmission of the SD-OCT signal is also demonstrated (**3**). A localized hyperautofluorescent spot in FAF at baseline and month 12 precedes drusen regression and the subsequent atrophy development at months 24 and 36 (*black arrows*). Please note that at month 24, FAF shows already focal loss of autofluorescence signal indicating atrophy development, whereas atrophy is not yet detectable in CFP.

reflectivity in the presence of atrophic areas. However, it was not tomographically located at the level of the choroid, but at the level of the inner retina as compared to other retinal areas in the same eye as the retina itself at the site of the lesion was elevated. Only later over time, the PED flattened and retinal thickness became markedly reduced with typical loss of outer retinal morphology. At the same time, the area size of the central lesion by en face imaging enlarged, showing a large central area with decreased FAF intensities. This additional type of atrophy development was not observed in study eyes in the cohort and was included as type 3 in the classification system (Table 3).

Discussion

This study demonstrates distinct phenotypic patterns for development of central retinal atrophy based on multimodal imaging findings in eyes with non–late-stage AMD that were considered at high risk for development of central atrophy. The results underscore the role of SD-OCT and cSLO imaging in earlier and more precise detection of atrophy compared with CFP alone.

The key observation of the current study is the detailed analysis and the distinction of three major types of development of central atrophy (i.e., cRORA), by multimodal imaging findings: spread of preexisting paracentral atrophy with subsequent central involvement [type 1]; de novo development with immediate localization in the macular center at first detection [type 2]; and flattening of a preexisting PED [type 3]). Further, three distinct precursor lesions were seen for type 2, namely large drusen ("nascent GA"), hyperpigmentary changes, and refractile deposits. These distinct phenotypes may indicate variations in the pathogenesis of atrophy development. A better understanding of atrophy development from different precursor lesions may also be helpful for the assessment of new therapeutic interventions and the development of new therapeutic strategies.

Due to the AREDS definitions, existing paracentral atrophy is not considered to be late AMD, and therefore encroaching of atrophy in the fovea by paracentral atrophy was included in the current study as type 1 for central atrophy development.[32] We would suggest, in accordance with the more recent AMD classification by Ferris and colleagues,[44] classifying any atrophy within the macula already as late AMD. Of note, BCVA decline was only moderate in the case of foveal involvement (mean –6.7 letters over a mean period of 2.6 years), similar to findings in previous studies.[13,45] Further, it can be assumed that paracentral atrophy may already be associated in dependence of the topography with severe visual disabilities in daily life (e.g., reading).

The systematic analysis of the longitudinal data recorded in the MODIAMD natural history study is in accordance with the view that large drusen are the most common precursor lesion for outer retinal atrophy development. In addition, we could confirm the recent observations by Wu et al. using SD-OCT imaging, who described features of so-called "nascent GA."[26] Furthermore, our findings suggest that abnormal FAF findings at the site of large drusen may be also prognostic for atrophy development while normal FAF intensities may indicate that

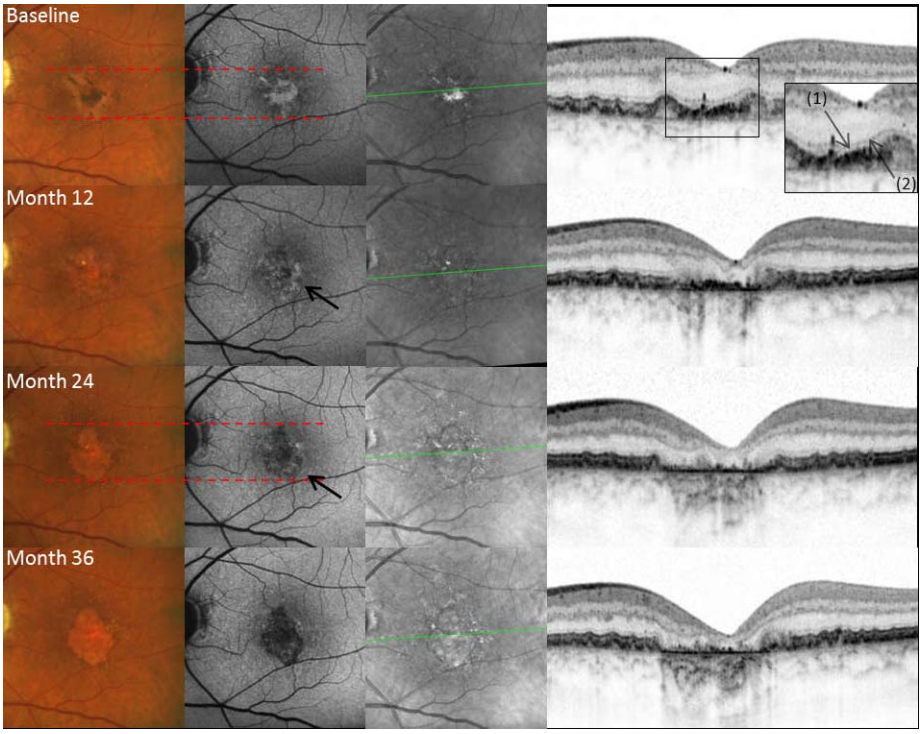

FIGURE 3. Illustration for development of central retinal atrophy in association with pigmentary changes without presence of large drusen (type 2b). Same arrangement of images as in Figure 1. SD-OCT imaging at baseline (baseline: *black box*) visit reveals hyperreflective material above the RPE/Bruch's membrane band (**1**), while the ELM is still continuous (**2**). The hyperpigmentary laminar lesion in CFP corresponds to a "patchy pattern" in FAF image (baseline: *red dashed lines*). Over the time, the initial increase in FAF signal becomes reduced, presenting an irregular area of more and more decreased FAF (months 12 and 24: *black arrows*). The atrophy-associated reduction in FAF shows a progredient inhomogeneous pattern with focal areas of hypoautofluorescence occurring first, while CFP image reveals more clearly the lesion's extent (month 24: *red dashed lines*).

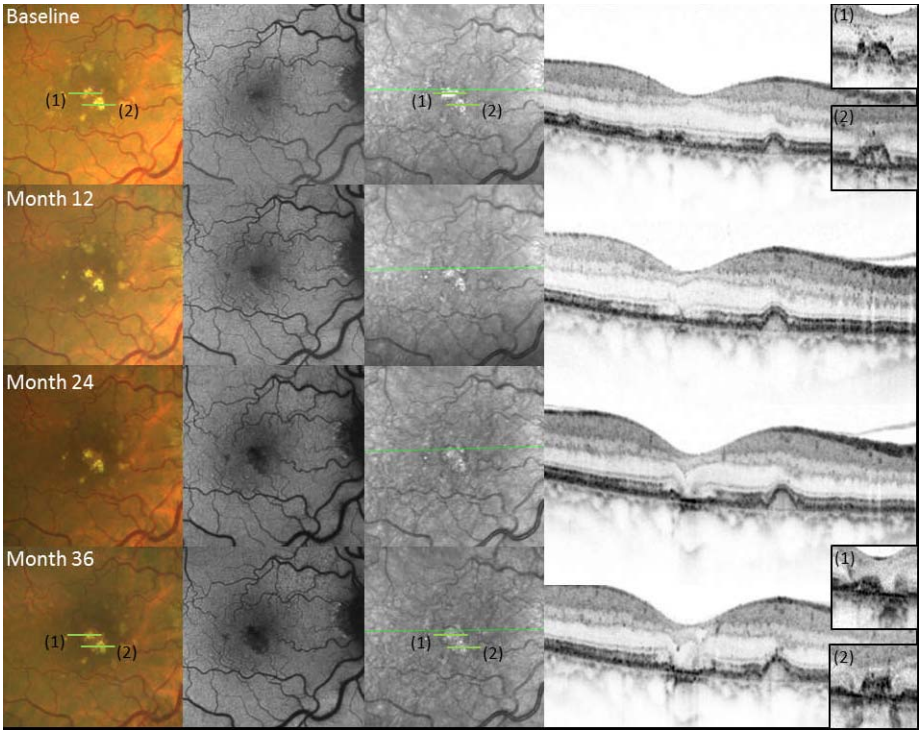

FIGURE 4. Example for development of central atrophy associated with refractile deposits (type 2c). Same arrangement of images as in Figure 1. At baseline and month 36, *small green lines* on CFP and NIR image indicate the position of the cropped SD-OCT scans (**1**) and (**2**) directly through the refractile lesions. At baseline and month 36, a pyramidal structure at the RPE level on top of the drusen ("ghost drusen") is visualized by SD-OCT, while CFP and NIR show clearly this feature originating from the refractile lesions.

Investigative Ophthalmology & Visual Science

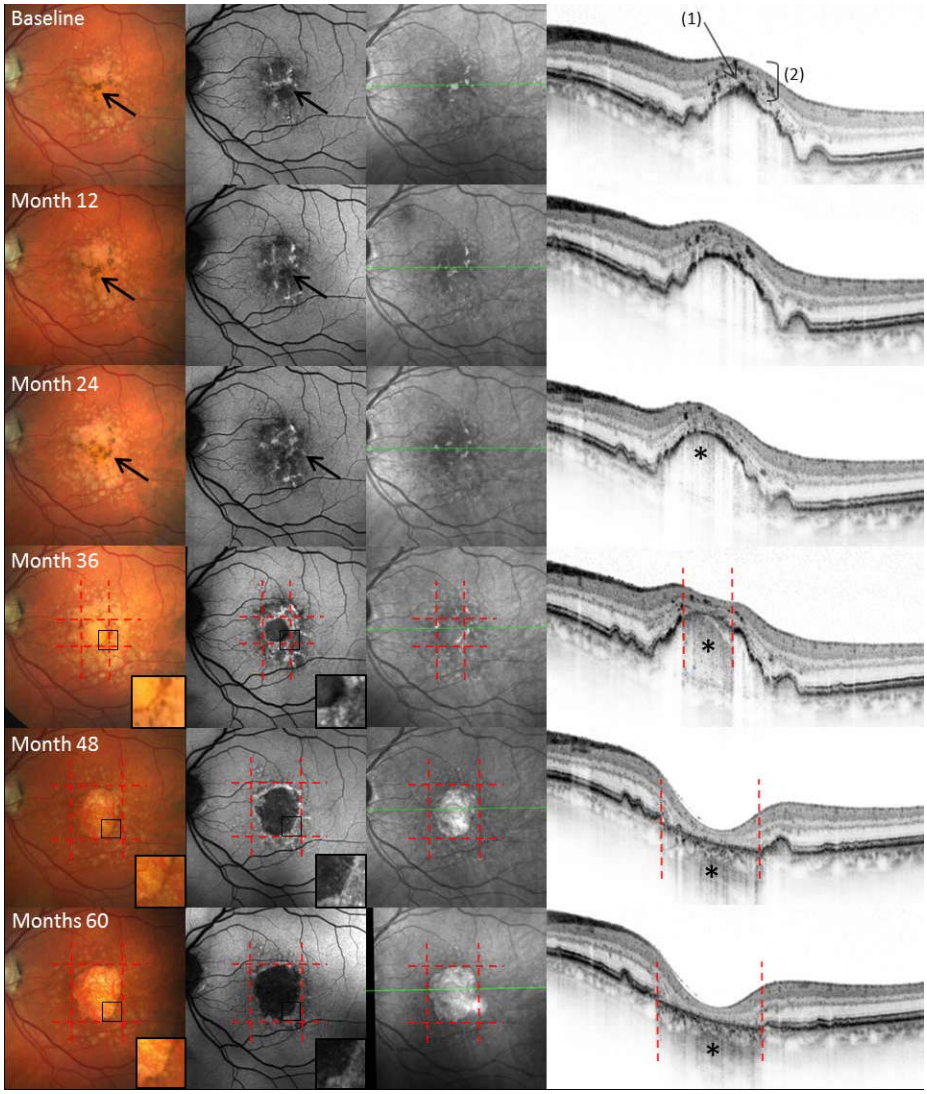

Figure 5. In one fellow eye, development of central atrophy was associated with flattening of a large pigment epithelium detachment (type 3). Same arrangement of images as in Figure 1. Extensive retinal hyperpigmentary changes, which resemble a cartwheel configuration, can be seen on CFP images starting at baseline (CFP images: *black arrows*). Corresponding to this hyperpigmentary changes-associated cartwheel configuration, FAF images show a similar pattern of hyper- and hypoautofluorescence (FAF images: *black arrows*). At baseline, a corresponding hyperreflective signal is detectable on top of the PED at RPE level (**1**) as well as numerous intraretinal hyperreflective foci (**2**). Over time, loss of hyperreflective foci along with disruption of the RPE on top of the PED and SD-OCT signal hypertransmission into the PED and further choroid (months 24–60: *black star*). Atrophy lesion extent is demonstrated by *red dashed lines* (months 36–60). Lesion borders showed a ring of hyperpigmentation in CFP and corresponding of hyperautofluorescence in FAF (months 36–60).

Table 3. Classification System of Central Atrophy Development Patterns

Phenotype	Study Eyes, $n = 17$	Fellow Eyes, $n = 3$
Type 1, spread of preexisting paracentral atrophy	6	1
Type 2, de novo development of central manifest atrophy, associated with:	(a) Large drusen	
	8	0
	(b) Pigmentary changes	
	1	1
	(c) Refractile deposits	
	2	0
Type 3, PED collapse	0	1

All eyes with iAMD at baseline of the MODIAMD study and development of central atrophy within 6 years are listed.

the "point of no return" to manifest atrophy has not yet been reached.

There have been only few reports on "primary age-related atrophy" without "obvious association with drusen," as described by Sarks et al.,[7] in the context of AMD. The AREDS reported "retinal hyperpigmentation" and "refractile drusen" as precursor lesions for atrophy development. However the analysis was based on CFP only over a period of 4 years, while the study herein provides an analysis by various imaging modalities over a 6-year review. In accordance with a more detailed detection of multimodal high-resolution imaging compared to solely CFP, the relative rate of central atrophy was higher in the current study (67% vs. 24%).[21] It may be speculated that these precursor lesions, although not as common as large drusen, are more definitely associated with atrophy development. For example, we have recently demonstrated that refractile deposits represented a high-risk factor for

late AMD development while large drusen may also regress without atrophy development.[22] No spatial association with the presence of RDR and development of cRORA over time has been detected over 6 years in this cohort.[31] Of note, the development of "outer retinal atrophy" in areas with RDR, also called subretinal drusenoid deposits, is typically not characterized by complete atrophy of the RPE and outer retinal layers.[46]

A major limitation for comparison of different studies is the use of inconsistent definitions of central atrophy. The AREDS definitions are based on CFP only and have been altered over time.[32,34] The AMD classification by Ferris and coworkers,[44] also based on CFP or clinical examination, does not define a minimum size of atrophy. Given the major technological advances in retinal imaging, more detailed classification and definition are prudent.[24] For this study, we adopted the recently proposed definition of cRORA that has been brought forward as part of the CAM program consensus classification system.[29] A better classification that becomes widely established would be also helpful for interpretation of other potential precursor lesions that have been recently described by SD-OCT, such as thinning of retinal layers in the presence of drusen regression, evolution of HRF, and disintegrated RPE dots. [23,26–28,47–51]

Various limitations of this study need to be considered. The number of included subjects is relatively small, and a substantial high number of subjects dropped out of this natural history study (a total of 32.7% at year 6). Therefore we cannot exclude that we missed other typical precursor lesions and patterns for atrophy development. For example, acquired vitelliform lesions were not included in this cohort. As patients exited the study at the time of either central atrophy by multimodal imaging or CNV development, further longitudinal data after such events were not systematically assessed. Therefore we cannot analyze the extent of the time lag for atrophy detection of CFP imaging as compared to the multimodal imaging approach. An important strength of the study is the prospective design of data acquisition within a natural history study employing extensive and standardized multimodal high-resolution retinal imaging at each study visit. This design was an important perquisite for the systematic analysis of different variations in the development and manifestation of central atrophy based on imaging findings beyond CFP.

In summary, the current study reports the incidence of central atrophy development secondary to AMD based on various imaging modalities. Three major precursor lesions for atrophy development were noted, and another three subphenotypes were additionally identified for de novo atrophy development. More detailed insights into atrophy development by multimodal longitudinal imaging may be helpful for a better understanding of the prognostic markers and in the context of future interventional clinical trials in patients with iAMD.

Acknowledgments

Supported by Federal Ministry of Education and Research of Germany (BMBF), Scholarship FKZ 13N10285, BONFOR GEROK Program, Faculty of Medicine, University of Bonn, Grant No. O-137.0026 (ST), and BONFOR GEROK Program, Faculty of Medicine, University of Bonn, Grant No. O-137.0022 and Grant No. O-137.0025 (MP).

Disclosure: **S. Thiele**, Carl Zeiss Meditec (F), Heidelberg Engineering (F), Optos (F); **M. Pfau**, Carl Zeiss Meditec (F), Heidelberg Engineering (F), Optos (F); **P.P. Larsen**, Novartis (F); **M. Fleckenstein**, Carl Zeiss Meditec (F), Optos (F), Genentech/Roche (F, R), Merz (C), Heidelberg Engineering (F, R), Novartis (R), Bayer (R), P; **F.G. Holz**, Allergan (C), Bayer (C), Heidelberg Engineering (C, F), Carl Zeiss Meditec (F), Optos (F); **S. Schmitz-Valckenberg**, Alcon/Novartis (C, F), Allergan (F), Bayer (F, R), Carl Zeiss MediTec (F), Formycon (F), Heidelberg Engineering (F, R), Optos (F), Genentech/Roche (C, F)

References

1. Wong WL, Su X, Li X, et al. Global prevalence of age-related macular degeneration and disease burden projection for 2020 and 2040: a systematic review and meta-analysis. *Lancet Glob Health*. 2014;2:e106–e116.
2. Rofagha S, Bhisitkul RB, Boyer DS, Sadda SR. Seven-year outcomes in ranibizumab-treated patients in ANCHOR, MARINA, and HORIZON: a multicenter cohort study (SEVEN-UP). *Ophthalmology*. 2013;120:2292–2299.
3. Bhisitkul RB, Desai SJ, Boyer DS, Sadda SR. Fellow eye comparisons for 7-year outcomes in ranibizumab-treated AMD subjects from ANCHOR, MARINA, and HORIZON (SEVEN-UP Study). *Ophthalmology*. 2016;123:1269–1277.
4. Grunwald JE, Daniel E, Huang J, et al. Risk of geographic atrophy in the comparison of age-related macular degeneration treatment trials. *Ophthalmology*. 2014;121:150–161.
5. Grunwald JE, Pistilli M, Ying G, Maguire MG, Martin DF; Comparison of Age-related Macular Degeneration Treatments Trials Research Group. Growth of geographic atrophy in the Comparison of Age-related Macular Degeneration Treatments Trials (CATT). *Ophthalmology*. 2015;122:809–816.
6. Maguire M, Martin D, Ying G, et al. 5-year outcomes with anti-VEGF treatment of neovascular age-related macular degeneration (AMD): the comparison of AMD treatments trials. *Ophthalmology*. 2016;123:1751–1761.
7. Sarks J, Sarks S, Killingsworth M. Evolution of geographic atrophy of the retinal pigment epithelium. *Eye (Lond)*. 1988; 2:552–577.
8. Gass JD. Drusen and disciform macular detachment and degeneration. *Arch Ophthalmol*. 1973;90:206–217.
9. Schmitz-Valckenberg S. The journey of "geographic atrophy" through past, present, and future. *Ophthalmologica*. 2017; 237:11–20.
10. Holz FG, Strauss EC, Schmitz-Valckenberg S, van Lookeren Campagne M. Geographic atrophy: clinical features and potential therapeutic approaches. *Ophthalmology*. 2014; 121:1079–1091.
11. Spaide RF. Improving the age-related macular degeneration construct: a new classification system [published online ahead of print May 26, 2017]. *Retina*. doi:10.1097/IAE.0000000000001732.
12. Holz FG, Bindewald-Wittich A, Fleckenstein M, Dreyhaupt J, Scholl HPN, Schmitz-Valckenberg S. Progression of geographic atrophy and impact of fundus autofluorescence patterns in age-related macular degeneration. *Am J Ophthalmol*. 2007; 143:463–472.
13. Sunness JS, Gonzalez-Baron J, Applegate CA, et al. Enlargement of atrophy and visual acuity loss in the geographic atrophy form of age-related macular degeneration. *Ophthalmology*. 1999;106:1768–1779.
14. Lindblad AS, Lloyd PC, Clemons TE. Change in area of geographic atrophy in the age-related eye disease study. *Arch Ophthalmol*. 2009;127:1168–1174.
15. Schmitz-Valckenberg S, Bindewald-Wittich A, Dolar-Szczasny J, et al. Correlation between the area of increased autofluorescence surrounding geographic atrophy and disease progression in patients with AMD. *Invest Ophthalmol Vis Sci*. 2006; 47:2648–2654.
16. Lindner M, Boker A, Mauschitz MM, et al. Directional kinetics of geographic atrophy progression in age-related macular degeneration with foveal sparing. *Ophthalmology*. 2015;122: 1356–1365.

17. Schmitz-Valckenberg S, Sahel J, Danis R, et al. Natural history of geographic atrophy progression secondary to age-related macular degeneration (Geographic Atrophy Progression Study). *Ophthalmology*. 2016;123:361–368.
18. Jaffe GJ, Schmitz-Valckenberg S, Boyer D, et al. Randomized trial to evaluate tandospirone in geographic atrophy secondary to age-related macular degeneration: the GATE study. *Am J Ophthalmol*. 2015;160:1226–1234.
19. Yaspan BL, Williams DF, Holz FG, et al. Targeting factor D of the alternative complement pathway reduces geographic atrophy progression secondary to age-related macular degeneration. *Sci Transl Med*. 2017;9:eaaf1443.
20. Grunwald JE, Pistilli M, Daniel E, et al. Incidence and growth of geographic atrophy during 5 years of comparison of age-related macular degeneration treatments trials. *Ophthalmology*. 2016;124:97–104.
21. Klein ML, Ferris FL, Armstrong J, et al. Retinal precursors and the development of geographic atrophy in age-related macular degeneration. *Ophthalmology*. 2008;115:1026–1031.
22. Oishi A, Thiele S, Nadal J, et al. Prevalence, natural course, and prognostic role of refractile drusen in age-related macular degeneration. *Invest Ophthalmol Vis Sci*. 2017;58:2198–2206.
23. Veerappan M, El-Hage-Sleiman A-KM, Tai V, et al. Optical coherence tomography reflective drusen substructures predict progression to geographic atrophy in age-related macular degeneration. *Ophthalmology*. 2016;123:2554–2570.
24. Holz FG, Sadda SR, Staurenghi G, et al. Imaging protocols in clinical studies in advanced age-related macular degeneration: recommendations from classification of atrophy consensus meetings. *Ophthalmology*. 2017;124:464–478.
25. Wu Z, Luu CD, Ayton LN, et al. Fundus autofluorescence characteristics of nascent geographic atrophy in age-related macular degeneration. *Invest Ophthalmol Vis Sci*. 2015;56:1546–1552.
26. Wu Z, Luu CD, Ayton LN, et al. Optical coherence tomography-defined changes preceding the development of drusen-associated atrophy in age-related macular degeneration. *Ophthalmology*. 2014;121:2415–2422.
27. Christenbury JG, Folgar FA, O'Connell RV, Chiu SJ, Farsiu S, Toth CA. Progression of intermediate age-related macular degeneration with proliferation and inner retinal migration of hyperreflective foci. *Ophthalmology*. 2013;120:1038–1045.
28. Schaal KB, Gregori G, Rosenfeld PJ. En face optical coherence tomography imaging for the detection of nascent geographic atrophy. *Am J Ophthalmol*. 2017;174:145–154.
29. Sadda SR, Guymer R, Holz FG, et al. Consensus definition for atrophy associated with age-related macular degeneration on OCT [published online ahead of print November 2, 2017]. *Ophthalmology*. doi:10.1016/j.ophtha.2017.09.028.
30. Steinberg JS, Gobel AP, Thiele S, Fleckenstein M, Holz FG, Schmitz-Valckenberg S. Development of intraretinal cystoid lesions in eyes with intermediate age-related macular degeneration. *Retina*. 2016;36:1548–1556.
31. Steinberg JS, Gobel AP, Fleckenstein M, Holz FG, Schmitz-Valckenberg S. Reticular drusen in eyes with high-risk characteristics for progression to late-stage age-related macular degeneration. *Br J Ophthalmol*. 2015;99:1289–1294.
32. Age-Related Eye Disease Study Research Group. The Age-Related Eye Disease study system for classifying age-related macular degeneration from stereoscopic color fundus photographs: the Age-Related Eye Disease Study Report Number 6. *Am J Ophthalmol*. 2001;132:668–681.
33. Schmitz-Valckenberg S, Göbel AP, Saur SC, et al. Automated retinal image analysis for evaluation of focal hyperpigmentary changes in intermediate age-related macular degeneration. *Trans Vis Sci Tech*. 2016;5(2):3.
34. Danis RP, Domalpally A, Chew EY, et al. Methods and reproducibility of grading optimized digital color fundus photographs in the Age-Related Eye Disease Study 2 (AREDS2 Report Number 2). *Invest Ophthalmol Vis Sci*. 2013;54:4548–4554.
35. Schmitz-Valckenberg S, Sadda S, Staurenghi G, Chew EY, Fleckenstein M, Holz FG. Geographic atrophy: semantic considerations and literature review. *Retina*. 2016;36:2250–2264.
36. Staurenghi G, Sadda S, Chakravarthy U, Spaide RF; International Nomenclature for Optical Coherence Tomography (IN OCT) Panel. Proposed lexicon for anatomic landmarks in normal posterior segment spectral-domain optical coherence tomography: the IN•OCT consensus. *Ophthalmology*. 2014;121:1572–1578.
37. Finger RP, Wu Z, Luu CD, et al. Reticular pseudodrusen a risk factor for geographic atrophy in fellow eyes of individuals with unilateral choroidal neovascularization. *Ophthalmology*. 2014;121:1252–1256.
38. Querques G, Querques L, Martinelli D, et al. Pathologic insights from integrated imaging of reticular pseudodrusen in age-related macular degeneration. *Retina*. 2011;31:518–526.
39. Schmitz-Valckenberg S, Brinkmann CK, Alten F, et al. Semi-automated image processing method for identification and quantification of geographic atrophy in age-related macular degeneration. *Invest Ophthalmol Vis Sci*. 2011;52:7640–7646.
40. Fleckenstein M, Schmitz-Valckenberg S, Adrion C, et al. Tracking progression with spectral-domain optical coherence tomography in geographic atrophy caused by age-related macular degeneration. *Invest Ophthalmol Vis Sci*. 2010;51:3846–3852.
41. Fleckenstein M, Issa PC, Helb HM, et al. High-resolution spectral domain-OCT imaging in geographic atrophy associated with age-related macular degeneration. *Invest Ophthalmol Vis Sci*. 2008;49:4137–4144.
42. Bonnet C, Querques G, Zerbib J, et al. Hyperreflective pyramidal structures on optical coherence tomography in geographic atrophy areas. *Retina*. 2014;34:1524–1530.
43. Balaratnasingam C, Yannuzzi LA, Curcio CA, et al. Associations between retinal pigment epithelium and drusen volume changes during the lifecycle of large drusenoid pigment epithelial detachments. *Invest Ophthalmol Vis Sci*. 2016;57:5479–5489.
44. Ferris FL III, Wilkinson CP, Bird A, et al. Clinical classification of age-related macular degeneration. *Ophthalmology*. 2013;120:844–851.
45. Schmitz-Valckenberg S, Fleckenstein M, Helb H-M, Issa PC, Scholl HPN, Holz FG. In vivo imaging of foveal sparing in geographic atrophy secondary to age-related macular degeneration. *Invest Ophthalmol Vis Sci*. 2009;50:3915–3921.
46. Spaide RF. Outer retinal atrophy after regression of subretinal drusenoid deposits as a newly recognized form of late age-related macular degeneration. *Retina*. 2013:1800–1808.
47. Curcio CA, Zanzottera EC, Ach T, Balaratnasingam C, Freund KB. Activated retinal pigment epithelium, an optical coherence tomography biomarker for progression in age-related macular degeneration. *Invest Ophthalmol Vis Sci*. 2017;58:BIO211–BIO226.
48. Monés J, Garcia M, Biarnés M, Lakkaraju A, Ferraro L. Drusen ooze: a novel hypothesis in geographic atrophy. *Ophthalmol Retin*. 2017;1:461–473.
49. Sleiman K, Veerappan M, Winter KP, et al. Optical coherence tomography predictors of risk for progression to non-neovascular atrophic age-related macular degeneration. *Ophthalmology*. 2017:124:1764–1777.

Investigative Ophthalmology & Visual Science

50. Ferrara D, Silver RE, Louzada RN, Novais EA, Collins GK, Seddon JM. Optical coherence tomography features preceding the onset of advanced age-related macular degeneration. *Invest Ophthalmol Vis Sci*. 2017;58:3519–3529.

51. Leuschen JN, Schuman SG, Winter KP, et al. Spectral-domain optical coherence tomography characteristics of intermediate age-related macular degeneration. *Ophthalmology*. 2013;120:140–150.

Investigative Ophthalmology & Visual Science